CHALLENGES IN EUROPEAN AEROSPACE
5TH CEAS AIR & SPACE CONFERENCE

CEAS

High-Speed PIV Applied to the Wake of the NASA CRM Model in ETW at High Re-Number Stall Conditions for Sub- and Transonic Speeds

Robert Konrath
German Aerospace Center (DLR)
Senior Scientist
Bunsenstrasse 10, Göttingen, 37073, Germany
Robert.konrath@dlr.de
Reinhard Geisler (DLR), Janos Agocs (DLR), Hauke Ehlers (DLR), Florian Philipp (DLR),
Jürgen Quest (European Transonic Windtunnel GmbH, ETW)

ABSTRACT

Within the framework of the EU project ESWIRP the Particle Image Velocimetry (PIV) using high-speed camera and laser has been used to measure the turbulent flow in the wake of a stalled aircraft wing. The measurements took place on the Common Research Model (CRM) provided by NASA in the pressurized cryogenic European Transonic Wind tunnel (ETW). A specific cryo-PIV system has been used and adapted for using high-speed PIV components under the cryogenic environment of the wind tunnel facility. First results are presented comprising transonic and subsonic stall conditions at realistic flight Reynolds numbers of 11.6 and 30 million, respectively.

1 INTORDUCTION

The flow on the suction side of an aircraft wing separates from all or part of the wing surface when a critical angle of incidence is reached, that depends on the current flow conditions. The separated flow regions produce highly unsteady and turbulent flow fields on the wing consisting large scale flow structures such as vortices [1,2]. The turbulent flow fluctuations propagate further downstream and can affect the flow around the empennage such that the effectiveness of control surfaces is reduced and, furthermore, due to their unsteadiness increased dynamic loads are induced. The characterization of the turbulent flow in the wake of a stalled wing is therefore of particular interest. The physics of the onset and evolution of flow separations as well as the produced unsteadiness and turbulence in the wake are not well understood. The prediction of such flows using CFD is still a challenging task making investigations in wind tunnels necessary. However, since the phenomena of flow separations strongly depend on the flow conditions it is crucial to closely match all important similarity parameters between the experiment and flight conditions requiring transonic Mach- and high Reynolds numbers in the range of M = 0.15 – 0.9 and R = 10 to 80 million, respectively.

On scaled aircraft models such extreme similarity flow parameters can be achieved simultaneously only in the European Transonic Wind tunnel (ETW) [3] located in Cologne, Germany and in the National Transonic Facility (NTF) at NASA Langley. Both facilities use a test gas of moderately compressed pure nitrogen at cryogenic temperatures. A sketch of the ETW facility is shown in Fig. 1. The 2.4 m wide and 2 m high test section is encapsulated by a large pressure shell of about 10 m in diameter. The plenum and wind tunnel circuit incorporate a pressure shell made of stainless steel that is internally cladded with insulation material. The compressed pure nitrogen gas reaches total temperatures of down to 110 K at total pressures of up to 450 kPa. However, due to the high operational costs of such wind tunnel

facilities, most investigations on aircraft models are performed in conventional wind tunnels at low Reynolds numbers.

The objective of the EU sub-project "Time-resolved wake measurements of separated wing flow and wall interference measurements" of ESWIRP (European Strategic Wind Tunnels Improved Research Potential) is to make a test campaign in the ETW possible in order to obtain instantaneous flow field data of the wake flow of an aircraft model at realistic sub- and transonic stall conditions [4]. For the investigations the Common Research Model (CRM) [5] has been chosen representing the geometry of a realistic aircraft. The wind tunnel model has been provided by NASA that has been already tested in the NTF in former campaigns. The obtained flow field data is used for further studies of the flow physics as well as to validate state-of-the-art CFD computations. The flow field measurements should be performed on the basis of an existing cryo-PIV system [6,7] that has been developed during the last years for applications in the ETW. Due to the specific conditions existing in the ETW a lot of problems arise when applying optical measurement techniques such as PIV making specific adaptations necessary. For the current tests high-speed PIV components have been integrated into this system resulting in a temporal resolution of 2 kHz in the velocity data.

The present paper focuses on the employed cryo-PIV setup for high speed flow field measurements that had been carried out within the framework of the ESWIRP project. Preliminary results from the wing wake at realistic Mach- and Reynolds numbers comprising sub- and transonic stall conditions, viz. at M = 0.25, R = 11.6 million and M = 0.85, R = 30 million, respectively, are presented.

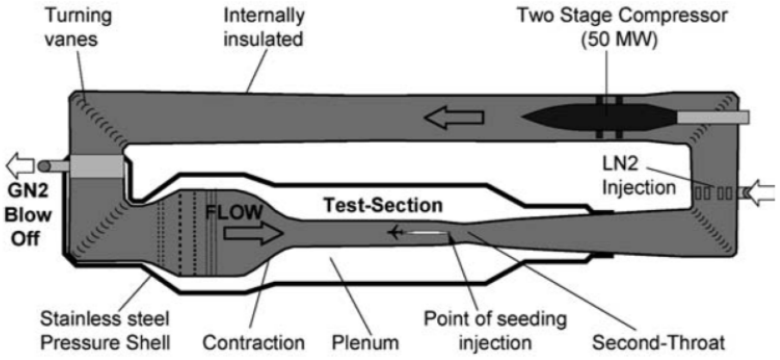

Figure 1: Sketch of the European Transonic Wind tunnel (ETW) facility for flight Mach and Reynolds number testing.

2 CRYO-PIV ARRANGEMENT FOR HIGH-SPEED PIV

2.1 Cryo-PIV system

The ETW test section is equipped with a number of window openings in the side walls as well as in the bottom and top walls behind which lamps and observation cameras can be installed, which is necessary since a pressure shell with a diameter of 10 m encloses the test section with limited optical access. The cryo-PIV system consists of special optical modules for a placement of cameras and light-sheet optics behind the test section windows. Because of the cryogenic environment, these modules are placed in heated housings. Since these components are no longer accessible once the wind tunnel is closed for a cool-down, necessary adjustments can be performed by remote control. Due to the extremely high operational costs of such a facility it is in particular essential that the whole measurement system and

controlling units operate reliably to avoid costly tunnel access. The cooling down or warming up of the wind tunnel takes several hours and consumes a huge amount of liquid nitrogen and electrical power.

The PIV laser is placed outside the wind tunnel and the laser beam is directed via laser mirrors through a small window in the plenum pressure shell to an optical module (containing the light-sheet-forming optics) installed in the test section wall. To compensate for laser light beam deflections caused by optical and mechanical effects when changing the tunnel temperature or pressure, a beam monitor is employed in this module which permits automatic repositioning and redirection of the laser beam using motorized mirrors placed inside the plenum via which the beam is directed to the entry window of the light-sheet module. Therewith, the beam is kept on the optical axis of the light sheet forming optics while the tunnel conditions change.

To produce flow tracers in the flow tiny ice crystals are used that are generated by injecting a small amount of water aerosol into the cryogenic environment of the wind tunnel. In contrast to oil droplets the ice crystals can be easily removed from the wind tunnel circuit by a warm-up without any risk to damage the internal porous insulation material. The formation of the ice crystals must be controlled carefully to produce tracers in the correct size ranging from about 0.5 to 2 µm; i.e. small enough to keep the lag between particle and flow velocities negligibly small and yet large enough for detectable light scattering off them using digital cameras. Their formation, growth and sublimation, however, depend on the dew point, pressure and temperature of the test gas. Also the amount of injected water must be kept small in order to preclude icing on the test section walls.

2.2 Employed High Speed PIV arrangement

The employed PIV arrangement in the ETW is shown in Figure 2. The light sheet is aligned parallel to the direction of the free stream velocity for a good dynamic range of the measured velocities. Because of the limited light energies of high-speed lasers operating at repetition rates in the order of 1 kHz and more (the current laser emits light of 10 mJ per pulse at a rate of 2 kHz) the light sheet width was limited to about 6 cm to achieve high enough light densities within the light-sheet. A light-sheet module containing the light-sheet forming optics and electronics for a remote control of the modules, is located in the bottom wall at a window in the middle row which is closest in position to the region of interest between the trailing edge of the wing and the tailplane. The different measurement positions are achieved by pivoting the light-sheet accordingly using rotatable laser mirrors inside the light-sheet module. By realizing two independent rotation axes the light sheet position could be varied independently in the streamwise and spanwise direction within the range of $\eta = 2\ y/b = 0.15$ to 0.5. A single camera module is placed in the side wall of the test section using a window that allows at most for a normal view to the light sheet planes at the different measurement positions. The field-of-view of the camera has been adjusted accordingly using a mirror setup inside the camera module. A PCO.dimax HS4 high-speed camera is used providing a sensor resolution of 1920 x 1080 Pixels at a frame rate of more than 4 kHz. This camera can be precisely triggered and is capable of re-cording two subsequent images with a short time separation of only 3.5 µs, which is just short enough for the measurement of the expected highest velocities for the transonic case.

The camera module and its installation inside the test section side wall are shown in Figure 3. Between the camera and the lens ($f = 200$ mm) a specific adapter is mounted, that incorporates three servo motors for a remote setting of the lens focus as well as the Scheimpflug axis and angle. All three degrees of freedom are necessary because of the varying three-dimensional orientation and position of the light sheet plane in order to get sharp particle images within the recorded pictures. The current field-of-view is set in the horizontal and vertical direction by using two motorized mirrors that are placed between the lens and the test section window. These mirrors are also used to compensate the Scheimpflug settings for which the lens had to be tilted since the camera is fixed with the module's frame due to its size and weight. The camera module also contains electronics for a full remote control and for

an image data transfer from the camera to a computer located in the wind tunnel control room via a fibre optic cable.

Figure 4 shows the installation of the light-sheet module in the bottom wall of the test section and the laser beam path via laser mirrors to the entry window of the housing.

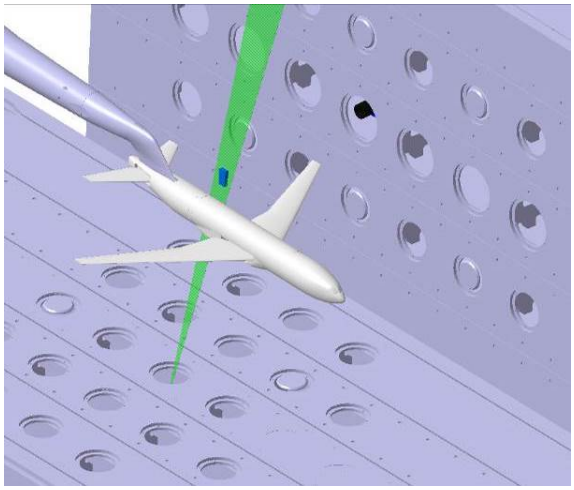

Figure 2: Sketch of the wind tunnel model (CRM, wing span *b* = 1.586 m) in the ETW test section (shown is only the bottom and side wall) along with the light sheet (green) and camera arrangement, the blue area indicate the field-of-view for the shown measurement position (for the tests the CRM model was rotated in an upside down position).

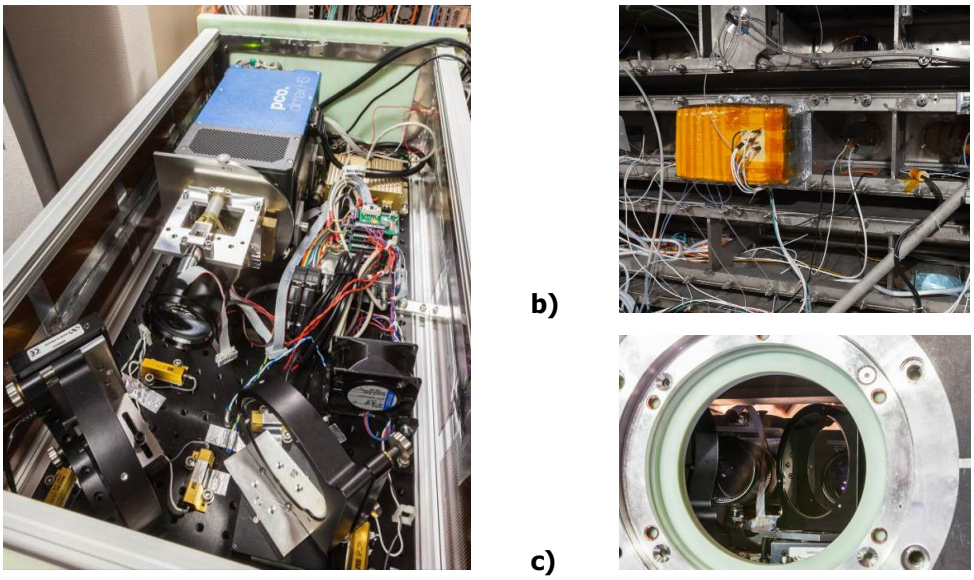

a) **b)** **c)**

Figure 3: Pictures of a) camera module inside housing b) rear side of test section with camera housing in place, c) view through window frame from inside the test section.

a) 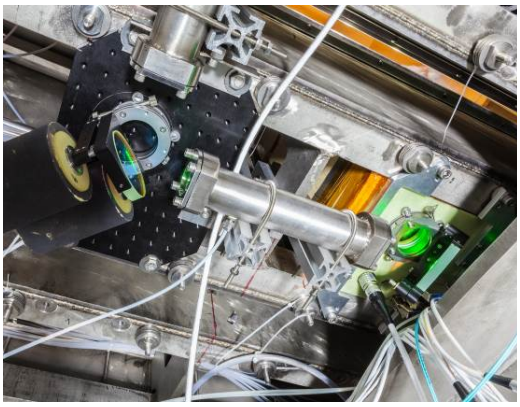 b) 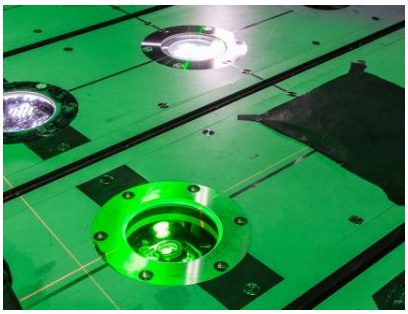

Figure 4: Pictures of light-sheet module installed inside bottom all of test section a) view of rear side seen from beneath the test section b) window of light sheet module inside the test section.

2.3 Data acquisition and processing

The extreme operational wind tunnel costs arising especially at transonic speeds due to the high consumption of liquid nitrogen and electrical power make it in particular essential to reduce the measurement times as much as possible. Therefore, the data acquisition has been automated using the software tool SemCollect featuring a link to the wind tunnel control system of the ETW, such that a PIV measurement can be triggered by the wind tunnel operator while performing an angle of attack polar (s. Fig. 5). Data of the current wind tunnel and model, the PIV system and image data are collected and stored automatically on a RAID storage system. The internal memory of the high-speed camera of 36 GByte allows for an acquisition of 7650 double-images. After each measurement capturing three series each of 2550 samples the image data is transferred from the camera to the data storage of the PIV system. Using the Camera-Link interface this took about 6 minutes, whereas the image recording was completed after 4 seconds. Just after the image data were available on the storage system, a fast on-line image evaluation was started using a matrix of 5 x 5 vector points at which the velocities are determined such that after about 5 minutes a statistical analysis comprising a time average, RMS values and frequency spectra of the velocities were available.

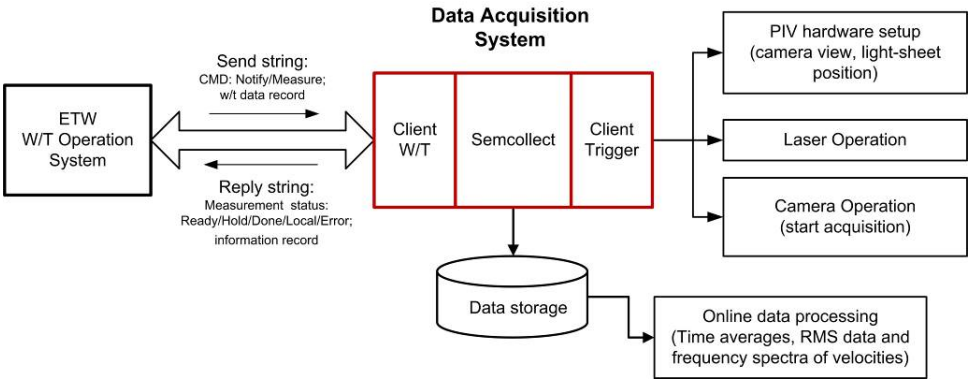

Figure 5: Automated data acquisition for high speed PIV measurements including an on-line data processing.

3 RESULTS

Below first results of a sub- and transonic stall are presented which are denoted by the polar numbers 304 and 313, respectively. The test parameters are summarized in Table 1. The span width of the CRM wind tunnel model is b = 1.586 m and the mean aerodynamic chord is c_{MAC} = 0.189 m. The PIV measurement plane was positioned within the wake of the wing as shown in Figure 6. The measurement positions of the polars 304 and 313 are at a spanwise position of about η = 60% of the wing half span and at about 1 and 1.2 mean aerodynamic chord lengths downstream the wing trailing edge.

Table 1: Test parameters of two PIV measurement cases.

Polar #	M	R, million	T_0, K	p_0, kPa	α, degs	$\eta = 2\,y_m/b$	$\xi = x_{TE}/c_{MAC}$
304	0.85	30	116	303	4.5	0.57	ca. 1.05
313	0.25	11.6	115	303	18	0.59	ca. 1.22

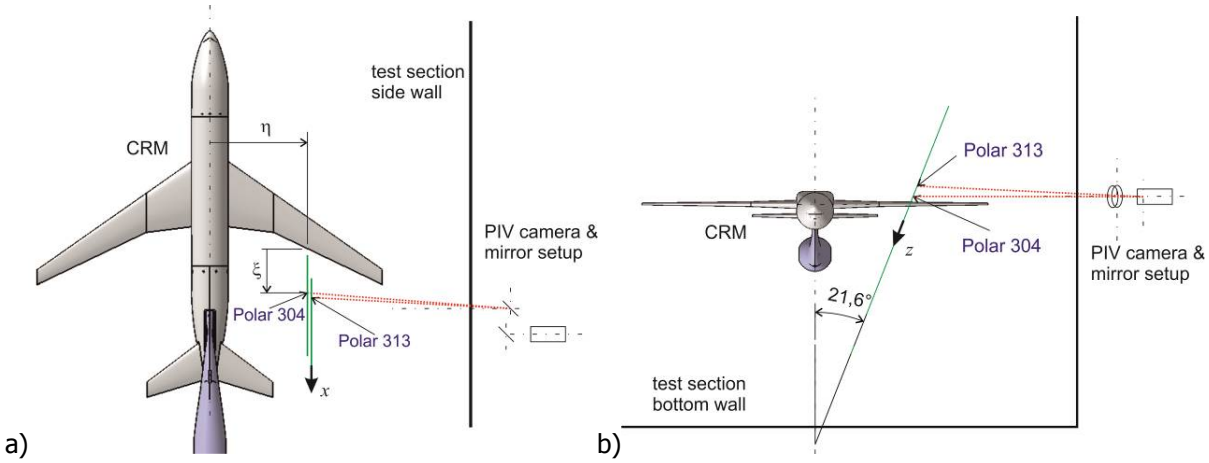

Figure 6: Arrangement of measurement plane within the test section using a) a bottom view and b) a front view looking in the direction of the free stream flow. The CRM wind tunnel model was measured in an upside down position and is shown for an incidence of zero degree. The green lines indicate the orientation of the light sheets for two measurement positions denoted by the Polar number. The dotted red lines indicate the direction of view and points to the origins of the used PIV coordinate system.

The used PIV *x*-coordinate of the measurement plane points in the direction of the free stream flow and the PIV *z*-coordinate has angle of 21.6 degs to the vertical axis of the test section as shown in Figure 6. The evaluation of the PIV images was complicated by regions in the images where blurred particle images occur caused by density changes in the flow that appear mainly in the transonic case reducing the spatial resolution and the precision in the velocities. In the subsonic case, flow regions with no detectable particle images, occurring primarily in the center of large vortex structures, leads to gaps in the velocity data. This has to be taken into account when interpreting the time averages and RMS values of the velocity fields. For the evaluation, a multi-grid algorithm6 with image-deformation has been applied using final interrogation window sizes of 64 x 64 pixels that correspond the 3.6 mm x 3.6 mm in the flow, whereas the spacing of the vectors is about 1.1 mm.

An instantaneous velocity field of the transonic stall case is shown in **Figure 7**. The wake of the stall region is characterized by high velocity fluctuations occurring mainly between z = -25 mm and z = 25 mm. From the velocity vectors shown in the right plot the free stream velocity of about 171 m/s is subtracted, such that vortical flow structures get visible in the wake region. The flow region below z = -25 mm shows very small variations and is situated downstream the pressure side of the wing.

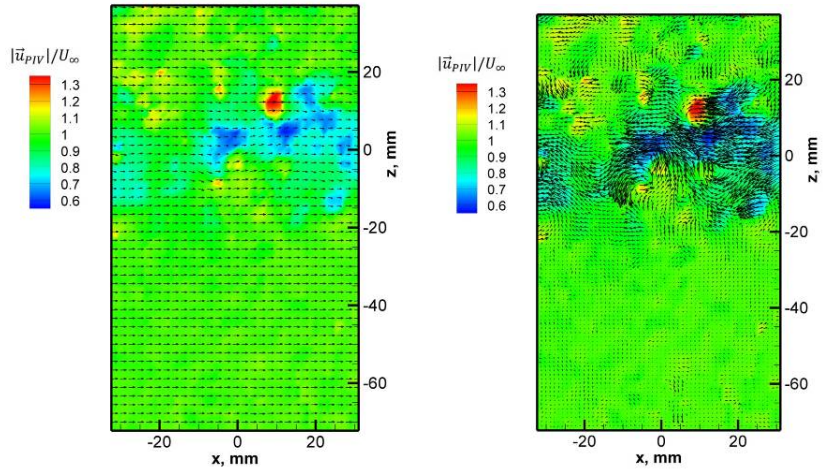

Figure 7. Instantaneous velocity field for the transonic stall condition of Polar 304 (M = 0.85, R = 30 Mio.) showing (left) absolute velocity vectors and (right) vectors relative to the free stream velocity.

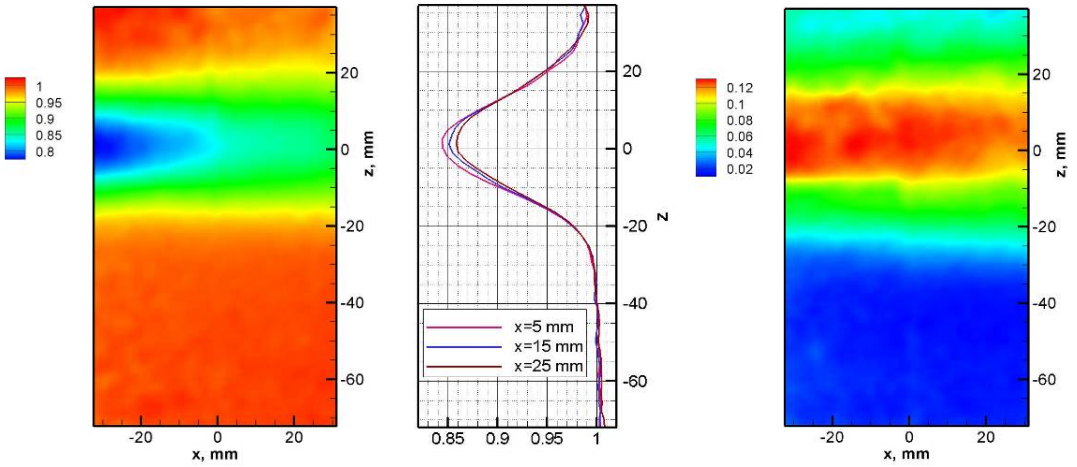

Figure 8. Contour plots of (left) time average of *u* and (middle) vertical *u* profiles and (right) RMS data of w using 7650 samples for the transonic stall condition of Polar 304 (M = 0.85, R = 30 Mio.).

The time average using 7650 velocity fields is shown in Figure 8 for the *u*-component. Also plotted are the vertical velocity profiles at three *x*-positions that show a maximum drop of u in the middle of the wake of about 15 % of the surrounding flow that is slightly decreasing in the downstream direction. The plot on the right shows the RMS values of the w-component with maximal values of about 12% of the time average.

Figure 9 shows a sequence of three velocity vectors fields of the subsonic stall case, from which again the free stream velocity has been subtracted, according to the maximum measurement rate of 2 kHz. The mainly backward directed flow velocity vectors in the upper part of the plots indicate the wake region downstream the flow separation on the wing suction side. In the lower third of the plot the shear

layer of the wake can be seen, where large scale vortices develop. Because of the lower free stream velocity in this case of about 54 m/s, flow structures and their development can be tracked inside the vectors fields with increasing time.

The time averages and RMS value distributions of the velocity vector fields are plotted in Figure 10 for the sub-sonic stall case. The lower shear layer can be identified in the time average contour plot of u by the boundary of the occurring velocity drop that is approximately located between z = -30 mm and z = -40 mm. A local minimum of about 50 % of the free stream velocity can be seen, where the RMS values of the w component reach about 40 % of the time average values.

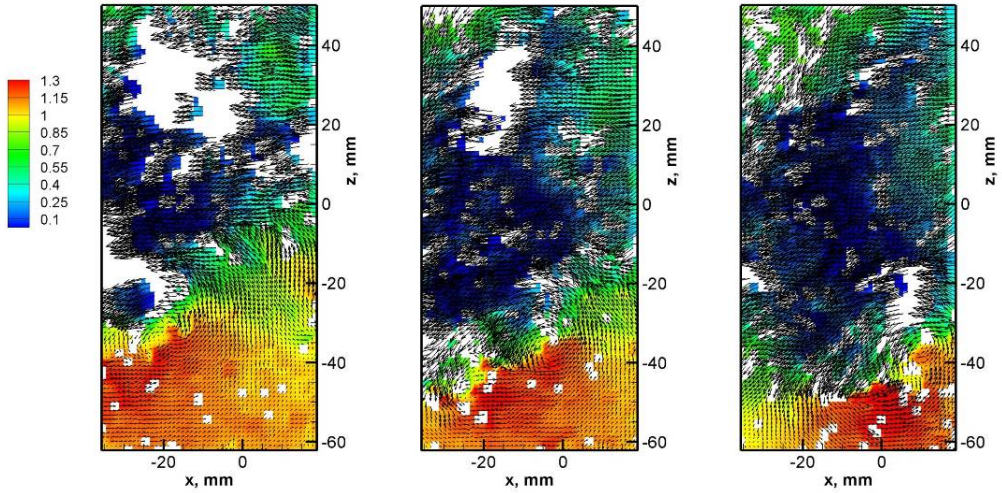

Figure 9. Instantaneous velocity fields for the subsonic stall condition of Polar 313 (M = 0.25, R = 11.6 Mio.) at three instances of time separated by 500 µs.

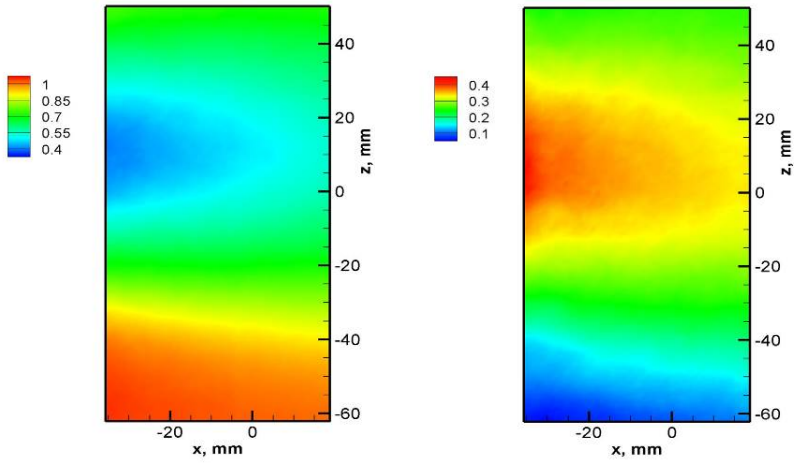

Figure 10. Contour plots of (left) time average of u and (right) RMS data of w using 7650 samples for the subsonic stall condition of Polar 313 (M = 0.25, R = 11.6 Mio.).

4 CONCLUSIONS

High speed PIV has been successfully applied to the wake flow of separated flow regions occurring on an aircraft wing at flight Mach and Reynolds numbers for sub- and transonic stall conditions. The measurements took place on the NASA's Common Research Model (CRM) in the European Transonic Wind tunnel (ETW). The cryogenic environment existing in the wind tunnel made it necessary to use an especially developed cryo-PIV system that has been equipped with a high speed camera allowing for measurement rates of 2 kHz. Due to the size and weight of the high speed camera a new housing and lens adapter have been constructed for these tests. The measurements have been performed at different spanwise and streamwise positions in the wing wake. The PIV data allow for investigations of the induced velocity fluctuations and their impact on the empennage of the aircraft at realistic conditions. Furthermore, the data are used for validations of CFD flow computations [8].

ACKNOWLEDGMENTS

The wind tunnel test campaign has been funded by the European Commission in the 7th framework program. The authors would like to acknowledge the EC for funding this research and the NASA for their readiness to provide the CRM wind tunnel model. The authors also would like to thank the ESWIRP coordinators and all partners involved in the wind tunnel campaign.

REFERENCES

[1] Seifert, A., Pack, L.G., "Oscillatory Excitation of Unsteady Compressible Flows over Airfoils at Flight Reynolds Numbers," 37th AIAA Aerospace Sciences Meeting and Exhibit, Reno NV, 11-14 Jan, AIAA 99-0925, 1999.

[2] Molton, P., Bur, R., Lepage, A., Brunet, V., Dandois, J., "Control of Buffet Phenomenon on a Transonic Swept Wing," 40th Fluid Dynamics Conference and Exhibit, 28 June – 1 July, Chicago, Illinois, AIAA 2010-4595, 2010.

[3] Quest J., Leuckert J., Fey U., Konrath R, and Egami Y., "Development & application of modern measurement techniques for pressurized cryogenic wind tunnels," Proc. of 26th International Congress of the Aeronautical Sciences, ICAS 2008, Anchorage (Alaska, USA), 14 - 19 September, CP-261, pp 1-12, 2008.

[4] Lutz, Th., Gansel, P.P., Godard, J.-L., Gorbushin, A., Konrath, R., Quest, J., Rivers, S.M.B., "Going for Experimental and Numerical Unsteady Wake Analyses Combined with Wall Interference Assessment by Using the NASA CRM Model in ETW," 51st AIAA Aerospace Sciences Meeting, AIAA 2013-0871, 2013.

[5] Rivers, M.B., Rudnik, R., Quest, J., "Comparisons of NTF, Ames and ETW results on the CRM," 53st AIAA Aerospace Sciences Meeting, 5 – 9 January, Kissimmee (FL / USA), Paper 2015-1093, 2015.

[6] Konrath, R., Agocs, J., Geisler, R., Otter, D., Roosenboom, E.W.M., Wolf, Th., Quest, J., "Flow Field Measurements by PIV at High Reynolds Numbers," 51st AIAA Aerospace Sciences Meeting, AIAA 2013-0869, 2013.

[7] Konrath, R., Agocs, J., Geisler, R., Otter, D., Roosenboom, E., Quest J.: Wing wake measurements at high Reynolds numbers by means of cryo PIV, Proc. of 10th Intern. Symp. on Particle Image Velocimetry – PIV13, Delft (NL), July 1-3, 2013.

[6] Raffel M., Willert C.E., Wereley S.T. and Kompenhans J., "Particle Image Velocimetry - A Practical Guide," 2nd Ed., Springer Berlin, ISBN 978-3-540-72307-3, 2007.

[8] Lutz, Th., Gansel, P.P., Waldmann, A., Zimmermann, D-M., Schulte am Hülse. S., "Time-Resolved Prediction and Measurement of the Wake Past the CRM at High Reynolds Number Stall Conditions," 53st AIAA Aerospace Sciences Meeting, 5–9 January, Kissimmee (FL / USA), AIAA 2015-1094, 2015.